

12-8-1997

# Cholesteric Gratings with Field-Controlled Period

Darius Subacius

Sergij V. Shiyanovskii

Philip J. Bos

*Kent State University - Kent Campus, pbos@kent.edu*

Oleg Lavrentovich

*Kent State University - Kent Campus, olavrent@kent.edu*

Follow this and additional works at: <http://digitalcommons.kent.edu/cippubs>

 Part of the [Physics Commons](#)

---

## Recommended Citation

Subacius, Darius; Shiyanovskii, Sergij V.; Bos, Philip J.; and Lavrentovich, Oleg (1997). Cholesteric Gratings with Field-Controlled Period. *Applied Physics Letters* 71(23), 3323-3325. Retrieved from <http://digitalcommons.kent.edu/cippubs/10>

This Article is brought to you for free and open access by the Department of Chemical Physics at Digital Commons @ Kent State University Libraries. It has been accepted for inclusion in Chemical Physics Publications by an authorized administrator of Digital Commons @ Kent State University Libraries. For more information, please contact [earicha1@kent.edu](mailto:earicha1@kent.edu), [tk@kent.edu](mailto:tk@kent.edu).

# Cholesteric gratings with field-controlled period

D. Subacius,<sup>a)</sup> S. V. Shiyonovskii,<sup>a)</sup> Ph. Bos,<sup>a),b)</sup> and O. D. Lavrentovich<sup>a),b)</sup>  
Kent State University, Kent, Ohio 44242

(Received 21 July 1997; accepted for publication 6 October 1997)

Diffraction gratings with period varied by an electric field are developed using a cholesteric liquid crystal confined between two transparent electrodes with unidirectionally treated alignment layers. In the initial state (zero field), the cholesteric layers are parallel to the cell planes. The electric field creates an in-plane modulated structure of variable period. Diffraction regimes of both Raman-Nath and Bragg types are demonstrated. © 1997 American Institute of Physics.  
[S0003-6951(97)01349-1]

Periodic helical arrangements of molecules in cholesteric liquid crystals lead to a variety of remarkable electrooptical phenomena that find applications in light modulators<sup>1-3</sup> and display devices.<sup>4</sup> Cholesteric cells have also a potential as electrically controlled diffractive gratings.

An ideal electrically-controlled cholesteric grating can be imagined as a uniformly modulated (in the plane of the grating) structure with a period that depends on the applied field. The possibility of the field-control period stems from the theoretical result that the helical pitch diverges when the field is applied normally to the helix axis of a cholesteric with positive dielectric anisotropy.<sup>5,6</sup> However, real samples are always bounded; surface anchoring can greatly modify the electrooptic response. Although the electrically-varying cholesteric periodicity is documented experimentally,<sup>7,8</sup> the surface alignment problems make it difficult to get simultaneously a uniform modulation and varying periodicity.<sup>9</sup> Thus optical diffraction phenomena are usually reported for cells with the so-called “fingerprint” nonuniform texture.<sup>10,11</sup> On the other hand, when a cell is designed as a uniform grating, it turns out that the period of modulations is practically field independent.<sup>12</sup> Chilaya *et al.*<sup>13</sup> reported recently on a very interesting effect of electrically-controlled color of cholesteric cells; however, neither the cholesteric structure nor the mechanism of the phenomenon have been revealed.

In this letter we describe a cholesteric grating that satisfies both conditions mentioned above: it is a unidirectional in-plane modulated structure with the period controlled by the field.

**Cell design and textures.** The cholesteric material is obtained by doping the nematic E7 (positive dielectric anisotropy  $\Delta\epsilon=13.8$  at  $f=1$  kHz, refractive indices  $n_0=1.522$ ,  $n_e=1.746$  at 20 °C) with the chiral agent CB 15 (both purchased from EM Industries, Inc.). The chiral mixture is sandwiched between two glasses with ITO electrodes. The electrodes are coated with polyimide SE-610 (Nissan Chem. Inc.) and rubbed unidirectionally to provide an in-plane “easy axis” of molecular orientation. While the modulations are caused by the field, it is the surface anchoring (due to the unidirectional rubbing) that keeps the uniformity of modulations in the plane of the cell. We describe two typical cells with different weight concentration  $c$  of the chi-

ral additive and thus different equilibrium pitch  $p$  of the cholesteric bulk (as reported by EM Industries, Inc.): No. 1 with  $c=17\%$ ,  $p=0.7\ \mu\text{m}$ , cell thickness (measured by the interference technique)  $d=2.3\pm 0.1\ \mu\text{m}$ ; and No. 2 with  $c=8.1\%$ ,  $p=1.7\ \mu\text{m}$ ,  $d=2.5\pm 0.1\ \mu\text{m}$ .

The zero-field state is a planar ( $P$ ) state with the cholesteric layers and molecules parallel to the cell substrates, Fig. 1(a). High-voltage  $U$  (ac sin-waves at  $f=1$  kHz,  $U>3.4$  V for cell No. 1 and  $>2.5$  V for cell No. 2) gives rise to a homeotropic ( $H$ ) state with molecules normal to the cell plates. By increasing the voltage applied to the  $P$  state or by decreasing the voltage applied to the  $H$  state, one obtains an  $M$  state modulated in the plane of the cell, Figs. 1(b), 2(a), 2(b). The period of modulations strongly depends on applied field, Figs. 2 and 3. The transition  $P-M$  is controlled by growth of oily streaks with cholesteric layers forming  $U$ -turns.<sup>14</sup> The  $H-M$  transition occurs via nucleation of rounded domains that transform into individual stripes which is similar to the process described for smectic  $A$  cells.<sup>15</sup> The stripes elongate by moving semicircular ends along the rubbing direction. Although the hysteresis effects are evidently in place, both field-increasing and field-decreasing regimes produce the  $M$  state with a field-controlled period, Fig. 2. For a naked eye, in the transmitted light, the  $M$  state has a uniform color that varies with the viewing angle and the voltage.

Both parameters  $p$  and  $d$  are important for proper design

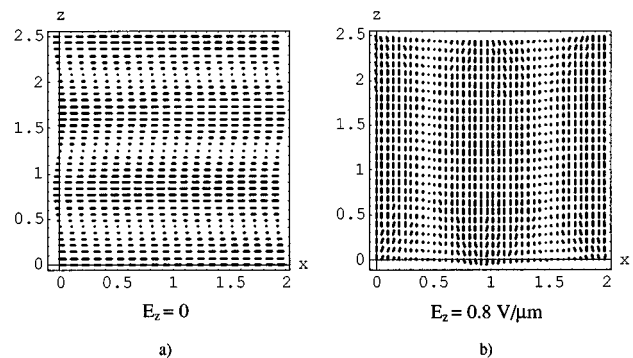


FIG. 1. Computer-simulated structure of a cholesteric liquid crystal (pitch  $p=1.7\ \mu\text{m}$ , elastic constants:  $6.4\times 10^{-12}$  N for splay,  $3\times 10^{-12}$  N for twist, and  $10\times 10^{-12}$  N for bend deformations;  $\Delta\epsilon=13.8$ ) in a cell with thickness  $d=2.5\ \mu\text{m}$  and unidirectional planar boundary conditions (polar anchoring coefficient  $4\times 10^{-5}$  J/m<sup>2</sup>, azimuthal anchoring coefficient  $2\times 10^{-5}$  J/m<sup>2</sup>): (a) initial planar orientation,  $P$  state,  $U=0$  V; (b) applied voltage  $U=2$  V,  $M$  state. The electric field is oriented along the axis  $z$ .

<sup>a)</sup>Liquid Crystal Institute.

<sup>b)</sup>Chemical Physics Program.

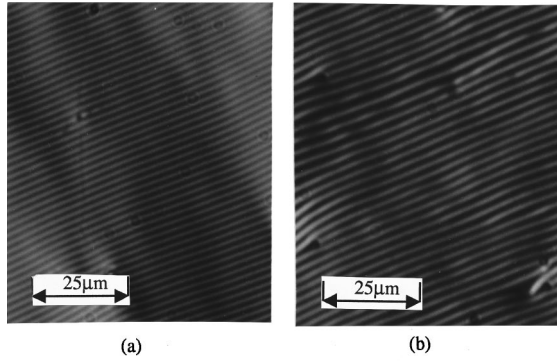


FIG. 2. Polarizing-microscope textures of the  $M$  state in cell No. 2 with modulations in the plane of the cell. The period of modulations changes with the applied voltage  $U$ : (a)  $U = 1.1$  V, (b)  $U = 1.75$  V.

of the grating. As described previously,<sup>9,12</sup> when  $d/p \approx 1$  and  $p \approx 5 \mu\text{m}$ , the grating orientation is not unique and the period changes very little with the field. In contrast, by raising the ratio  $d/p$ , we obtain the  $M$  grating with unique orientation and field-dependent period. Computer simulations based on Frank–Oseen elasticity with dielectric and Rapini–Papoular surface anchoring terms<sup>16</sup> were used to mimic the  $M$  structure. Figure 1(b) shows the simulated structure obtained for parameters close to that of the cell No. 2. In the bulk, the structure remains helicoidal with slightly nonsinusoidal (due to the applied field) director twist. Near the surfaces, complicated three-dimensional distortions occur.

**Light Diffraction.** Diffraction studies were performed at room temperature with He-Ne laser ( $\lambda = 633$  nm), mainly for the  $M$  state obtained from the  $H$  state. Polarization of the incident light was set by a rotating polarizer. The cell was mounted on a rotating stage.

The  $M$  state is the polarization-sensitive phase diffraction grating; only the component of light polarized along the rubbing direction, which is the direction of grating stripes,<sup>12</sup> is scattered. The scattering plane is normal to this direction.

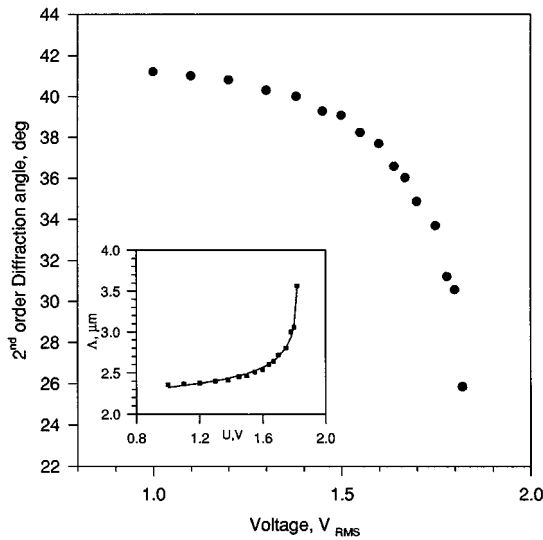


FIG. 3. Direction of the second diffraction maximum and the grating period  $\Lambda$  [calculated from Eq. (2)] as the function of the voltage applied to the cell No. 2. Experimental data  $\Lambda(U)$  are fitted by Eq. (3) with  $U_C = 1.85$  V ( $U_C = E_C \cdot d$ ) and equilibrium pitch  $p = 1.95 \mu\text{m}$ .

It is customary to distinguish two types of diffraction, depending on the parameter<sup>17</sup>

$$Q = \frac{2\pi \cdot \lambda L}{n\Lambda^2}, \quad (1)$$

where  $L$  is the thickness of the grating,  $\Lambda$  is the grating period and  $n$  is the spatially averaged refractive index of the diffractive medium. A “thick” grating,  $Q \gg 1$ , corresponds to Bragg diffraction and can produce a strong diffraction maximum when the incident angle satisfies the phase-matching condition.<sup>17</sup> Here and below we measure all the angles from to the normal to the cell. “Thin” grating,  $Q \ll 1$ , determines the Raman–Nath diffraction. For normal incidence, the directions of the diffraction orders  $m = 0; \pm 1; \pm 2, \dots$  are

$$\theta_m = \arcsin(m\lambda/\Lambda). \quad (2)$$

The  $M$  state is capable of diffraction in both regimes.

*Cell No. 1* shows Bragg diffraction. With fixed  $\lambda = 633$  nm, the intensity of the diffracted beam strongly depends on the angle of incidence and reaches a maximum when the incident angle is equal to the Bragg angle.<sup>17</sup> The diffraction angle  $\theta_d$  changes with  $U$ :  $\theta_d = 35.5^\circ$  at  $U = 3.15V_{\text{rms}}$ ,  $\theta_d = 41^\circ$  at  $U = 2.67V_{\text{rms}}$ , and  $\theta_d = 48.8^\circ$  at  $U = 1.9V_{\text{rms}}$ . In other words, for each value of  $U$ , the incident angle should be adjusted to satisfy the Bragg condition.<sup>17</sup> The maximum efficiency of diffraction (calculated with respect to the incident light intensity) is  $\approx 0.3$  and does not change significantly with  $U$ . The diffraction corresponds to the basic period related to  $p/2$  (the actual period is higher than  $p/2$ ). In addition, a much weaker (by two orders of magnitude) diffraction maximum related to a double period is also observed. We attribute this maximum to the symmetry-breaking effect of the bounding plates.<sup>12,18</sup> Note finally that all the diffraction efficiencies reported in this article are measured for cells that are not optically optimized for maximum efficiency.

*Cell No. 2* shows Raman–Nath diffraction with visible  $0, \pm 1, \pm 2, \pm 3$  diffraction orders for a beam incident normally to the cell. Figure 3 shows the voltage dependencies of the diffraction angle of the main maximum (second order) and grating period  $\Lambda$ , that corresponds to the distance between the stripes in Fig. 2. The field dependence of  $\Lambda$  produces a beam steering effect: with the fixed incident beam, a variation of  $U$  results in a continuous deflection of the diffracted beam (within an angular sector about  $20^\circ$ ). Note that defects of the  $M$  texture, Fig. 2, cause light scattering around the diffraction angle with a scattering cone angle of about  $3^\circ\text{--}4^\circ$ .

Figure 4 illustrates how the applied voltage changes the diffracted intensity for the zeroth-, first-, and second-order maxima. Near the  $M$ – $H$  transition the intensity of the first-order maxima increases and becomes comparable with the intensity of the second-order maxima.

The time response of the  $M$ – $H$  transition is of the order of 10 ms. Complete  $H$ – $M$  relaxation takes seconds. The  $M$ – $P$ – $M$  transitions are somehow slower:  $M$ – $P$  takes about 0.2 s and  $P$ – $M$  about 2 s.

To conclude, we have demonstrated that simultaneous action of dielectric reorientation and unidirectional surface

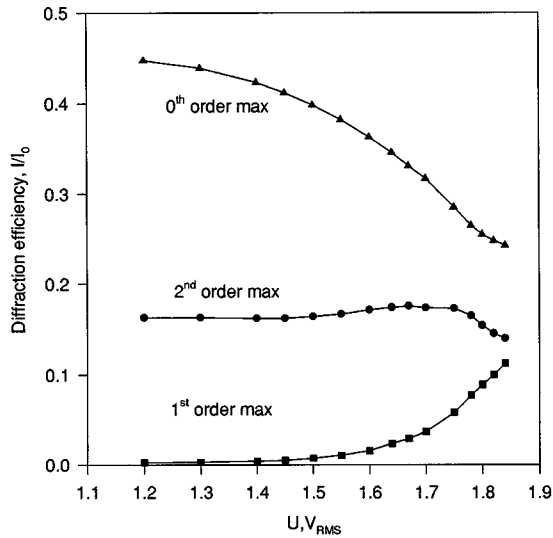


FIG. 4. Intensities of the zeroth-, first-, and second-order diffraction maxima as the functions of the voltage applied to the cell No. 2.

anchoring produces a uniform modulated state in the plane of the cholesteric cell. This  $M$  state is a phase grating capable of both Bragg and Raman–Nath diffraction. The regime of diffraction can be selected by adjusting the cell thickness and the cholesteric pitch. The crucial feature is that the field changes the modulation period thus providing continuous beam steering in the device with no mechanically moving elements. The control of the variable-grating cell is provided by a low-voltage ac field, in contrast to modulated nematic devices<sup>18</sup> operated by a high-voltage dc field.

The mechanisms of formation of the  $M$  state from both the planar and the homeotropic states present a new and interesting physical problem. For example, the  $P$ – $M$  transition and the variation of the period do not fit the well-known Helfrich–Hurault model of field-induced layer undulations in the planar cell.<sup>19</sup> Qualitatively, one can relate the period variation to the phenomenon of field-induced unwinding of an ideal cholesteric helix. For an unbounded cholesteric, the pitch diverges as<sup>5,6,19,20</sup>

$$p \propto - \sqrt{\frac{4\pi K_{22}}{\Delta\epsilon}} \frac{1}{E} \ln\left(1 - \frac{E}{E_C}\right), \quad (3)$$

where  $K_{22}$  is the twist elastic constant,  $E$  is the applied electric field, and  $E_C$  is the critical field of the cholesteric–nematic transition. Despite the fact that Eq. (3) gives a good fit of the experimental  $\Lambda(U)$  dependence (solid line in Fig. 3), the applicability of Eq. (3) to the bounded samples is obviously limited because of the finite surface anchoring. The detailed director structure of the  $M$  state, its dependence on the applied field, and the defect-mediated transitions  $M$ – $P$  and  $M$ – $H$  remain to be studied.

The authors thank G. Chilaya and D. Krueker for Ref. 13. This work was supported by BMDO/AFOSR under Grant No. F49620-96-1-0449 and by NSF STC ALCOM under Grant No. DMR-20147.

- <sup>1</sup>M. Schadt and W. Helfrich, *Appl. Phys. Lett.* **18**, 127 (1971).
- <sup>2</sup>C. S. Wu and S.-T. Wu, *Proc. SPIE* **1665**, 250 (1992).
- <sup>3</sup>K. A. Crandall, M. R. Fisch, R. G. Petschek, and Ch. Rosenblatt, *Appl. Phys. Lett.* **64**, 1741 (1994).
- <sup>4</sup>D. K. Yang and J. W. Doane, *SID International Symposium*, May 1992, p. 759.
- <sup>5</sup>P. G. de Gennes, *Solid State Commun.* **6**, 163 (1968).
- <sup>6</sup>R. B. Meyer, *Appl. Phys. Lett.* **12**, 163 (1968).
- <sup>7</sup>F. J. Kahn, *Phys. Rev. Lett.* **24**, 209 (1970).
- <sup>8</sup>C. J. Gerristma and P. van Zanten, *Phys. Lett. A* **37**, 67 (1971).
- <sup>9</sup>V. G. Chigrinov, V. V. Belyaev, S. V. Belyaev, and M. F. Grebenkin, *Sov. Phys. JETP* **50**, 994 (1979).
- <sup>10</sup>E. Sackmann, S. Meiboom, L. C. Snyder, A. E. Meixner, and R. E. Dietz, *J. Am. Chem. Soc.* **90**, 3567 (1968).
- <sup>11</sup>M. Kawachi, K. Kato, and O. Kogure, *Jpn. J. Appl. Phys.* **17**, 1245 (1978).
- <sup>12</sup>D. Subacius, Ph. Bos, and O. Lavrentovich, *Appl. Phys. Lett.* **71**, 1350 (1997).
- <sup>13</sup>G. Chilaya, G. Hauck, H. D. Koswig, and D. Sikharulidze, *J. Appl. Phys.* **80**, 1970 (1996).
- <sup>14</sup>M. Kléman, *Rev. Mod. Phys.* **52**, 555 (1989).
- <sup>15</sup>Z. Li and O. D. Lavrentovich, *Phys. Rev. Lett.* **73**, 280 (1994).
- <sup>16</sup>P. G. de Gennes and J. Prost, *The Physics of Liquid Crystals* (Clarendon, Oxford, 1993).
- <sup>17</sup>A. Yariv and P. Yeh, *Optical Waves in Crystals* (Wiley, New York, 1984), p. 356.
- <sup>18</sup>A. R. Tanguay, Jr., C. S. Wu, P. Chavel, T. C. Strand, A. A. Sawchuk, and B. H. Soffer, *Opt. Eng. (Bellingham)* **22**, 87 (1983).
- <sup>19</sup>S. A. Pikin, *Structural Transformations in Liquid Crystals* (Gordon and Breach, New York, 1991) (Translated from Soviet Edition, Nauka, Moscow, 1981).
- <sup>20</sup>S. V. Shiyonovskii and Ju. G. Terentiev, *Liq. Cryst.* **21**, 645 (1996).